

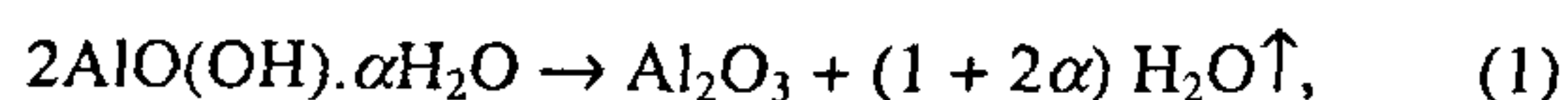
Fast surface oxidation induced growth of $\text{AlO}(\text{OH}) \cdot \alpha\text{H}_2\text{O}$ molecular fibres at nascent Al-metal surface in ambient atmosphere

S. Ram* and S. Rana

Materials Science Centre, Indian Institute of Technology, Kharagpur 721 302, India

The conditions are explored for an activated surface oxidation of nascent Al-metal surface in $\text{AlO}(\text{OH}) \cdot \alpha\text{H}_2\text{O}$ molecular fibres in air. It is found that a surface treatment of the specimen by a surface catalyst of Hg^{2+} -cations promotes its oxidation in air by an activated diffusion of the reaction species at ambient temperature. In this process, H_2O molecules from the air decompose readily into nascent H^+ and OH^- ions at the nascent Al-metal surface created by a peculiar surface reaction of Hg^{2+} -cations over it. The nascent OH^- ions instantaneously recombine with Al atoms at the Al-metal surface by electron transfer reaction, forming an oxidized product of latter, $\text{AlO}(\text{OH}) \cdot \alpha\text{H}_2\text{O}$ in the form of fibres. Three primary forces (i) the chemical potential between the reaction species, (ii) the fast diffusion of the reaction species, and (iii) the mechanical stress caused in expansion of the specimen during the reaction, drive the growth of fibres in a common direction perpendicular to a Al-metal surface. It presents a simple and cost-effective method to yield the product of Al_2O_3 derivatives.

$\text{AlO}(\text{OH}) \cdot \alpha\text{H}_2\text{O}$ is a precursor of alumina (Al_2O_3) or sapphire, which is one of the most important high-tech ceramic materials with exceptional properties such as greater hardness, chemical inertness, and a high melting temperature¹⁻³. On heating at 500 K or higher in air, it readily transforms to Al_2O_3 ,



with an insignificant change in its bulk shape according to the experimental conditions. This is highly important in fabricating its fibres with a uniform thickness. Al_2O_3 fibres are well-known fillers for forming reinforced metal matrix^{4,5} as well as ceramic and/or polymer matrix composites⁶⁻⁸ of superior structural and mechanical properties. The latter have been used extensively in aerospace and automobile industries as a high strength, high stiffness, and lightweight alternative to aluminum and titanium metals. High raw material costs, unavailability of well-known processing techniques, insufficient ex-

posure to technology and tradition are the main barriers for implementation of products in most of the applications.

The synthesis of pure Al_2O_3 fibres is presently too expensive for wide commercial use^{1,9}. In an attempt to reduce the manufacturing costs, a variety of modifications and synthesis route are being developed to make composite fibres^{9,10}. These fibres are usually produced by primarily using a spinning (of the melt or an aqueous mixture of the precursors) or a sol-gel method^{9,10}. The melt/precursor in the first method requires viscoelastic properties to permit the spinning of fibres. It therefore limits the compositions to only those which provide necessary forming properties. Thus a reasonably high percentage of glass former is admixed in a sample to support the formation of fibres⁹. The sol-gel method does not necessarily use a glass former additive in the final fibre. However, in this case also, the material is often biphasic with impurities of a soft glassy phase¹⁰. The glassy phase softens at an elevated temperature and deteriorates the high strength and other properties of the fibres.

In this article, we explore surface oxidation of Al-metal in air as a new chemical route for synthesizing $\text{AlO}(\text{OH}) \cdot \alpha\text{H}_2\text{O}$ molecular fibres of its oxidized product. The observation is an activated self-induced oxidation of nascent Al-metal surface in air and catalysed with a surface catalyst of Hg^{2+} -cations^{11,12}. Its valence readily changes from Al to Al^{3+} with a unidirectional growth of the latter in separated fibres. The chemical potential between the reaction species and expansion of the specimen during the reaction drive is directed perpendicular to the Al-metal surface. The uniqueness of this method is that it does not use a precursor or a glass former additive in any stage of the reaction and also does not involve even a container that often is a source of impurities in other methods. The preliminary results are presented with the study of the process of growth, microstructure, and composition of the fibres.

Experimental details

The proposed surface oxidation reaction of Al-metal was carried out with high purity (99.99%) Al-metal foils

*For correspondence (e-mail: sram@matssc.iitkgp.ernet.in)

from Goodfellow. The foil was degreased, washed in distilled water, and treated with 0.1 M HCl for 10 min followed by washing in water again. It yielded a refreshed Al-surface, which still has a very thin oxidized surface film that does not permit their reaction with air at room temperature (RT). An activated reaction occurs if the specimen is treated with a surface catalyst of Hg^{2+} -cations. In this process, the specimen is dipped in an aqueous 0.1 M Hg^{2+} solution for ~ 30 s and then rinsed properly with distilled water. The Hg^{2+} -cations react with the Al atoms on the Al-surface by forming a thin amalgam. The amalgam adheres to the nascent Al-surface, the surface oxide film and byproduct impurities (formed during its processing) segregate over it. The excess amalgam and other unwanted surface impurities are removed by washing the specimen in distilled water.

The specimen obtained has nascent Al-surface. If put in open air, they instantaneously react and form a surface oxidized product of the Al-metal in $\text{AlO}(\text{OH}) \cdot \alpha\text{H}_2\text{O}$ molecular fibres. This involves a self-induced spontaneous exothermic reaction. The fibres grow in a self-organized manner at the Al-metal surface perpendicular to it.

The morphologies of the $\text{AlO}(\text{OH}) \cdot \alpha\text{H}_2\text{O}$ fibres, which were grown under different experimental conditions at the Al-metal surface, were studied by taking their photographs. Their X-ray diffractograms were recorded with a P.W. 1710 diffractometer using a filtered $\text{Co K}\alpha$ radiation of wavelength $\lambda = 0.17904$ nm. A JEOL model-840 scanning electron microscope (SEM) was used to study their average diameter and was also used for an *in situ* elemental analysis. The elemental analysis gives a better purity of the sample than 99.9%.

Thermogravimetric analysis was carried out by heating the $\text{AlO}(\text{OH}) \cdot \alpha\text{H}_2\text{O}$ fibres over 300–850 K with the help of a Perkin–Elmer thermal analyser. Its bulk density was measured very precisely, accurate to a second decimal place, using the Archimedes' principle in N_2 gas with the help of a Penta Pyknometer (supplied by Quanta Chrome USA). Other experimental details were the same as reported elsewhere^{11,12}.

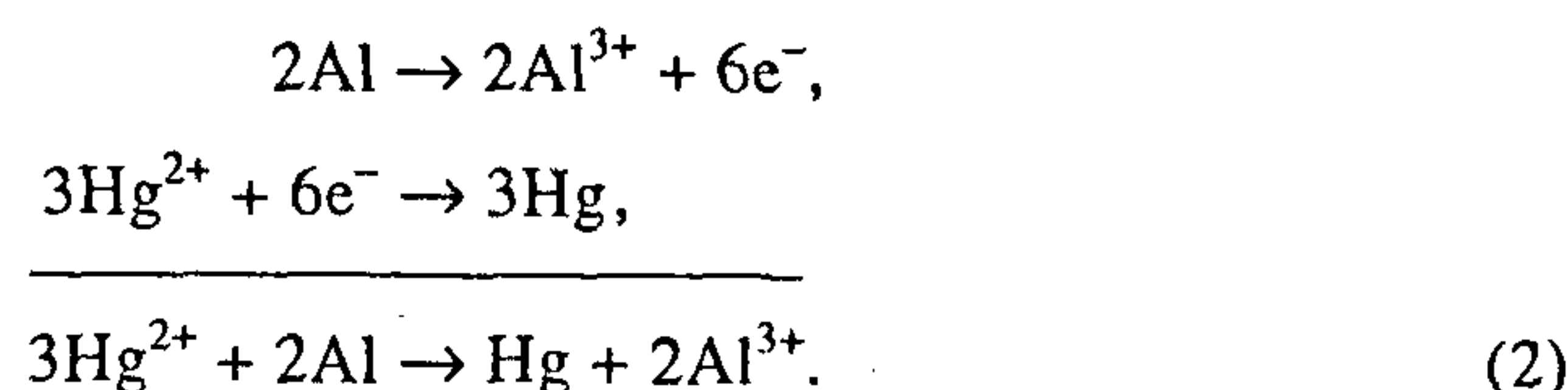
Results and discussion

Process of growth and structure of fibres

On treating with Hg^{2+} -cations the Al-metal surface adds a thin Hg^{2+} -surfactant layer over it with a thin Al- Hg^{2+} interface of possibly a monoatomic thickness¹¹. It was observed that in this process the Hg^{2+} -cations have a strong exothermic surface reaction with the Al-metal surface. Thus this reaction occurs instantaneously and lasts over a short time interval of about 100 s from the moment the two reaction species are put in contact and an intimate Al- Hg^{2+} interface is formed. The heat released

raised the average temperature (initially at $T_1 = 295$ K) of the sample by as much as $\Delta T = 10$ K without external cooling and insulation of the sample. The value of ΔT depends upon T_1 and other experimental conditions. Accordingly, we assume that the Al atoms in the interface instantaneously co-reduce Hg^{2+} -cations into Hg-metal in the interface. The latter forms a thin amalgam film with Al atoms at the interface. The virgin amalgam film is thin as possible so that it is not visible in an optical microscope or in an SEM.

The $\text{Hg}^{2+} \rightarrow \text{Hg}$ co-reduction reaction by the Al atoms at the nascent Al-metal surface can be described as follows,



It is an electrochemically feasible reaction with a positive ($\phi = 0.851$ V) value of chemical potential per $\text{Hg}^{2+} + 2\text{e}^- \rightarrow \text{Hg}$ reaction if compared with a negative $\phi = -1.662$ V value in the $\text{Al}^{3+} + 3\text{e}^- \rightarrow \text{Al}$ reaction¹³. In order to confirm the validity of this reaction, in a separate experiment, we successfully co-reduced a Hg^{2+} -salt into a pure Hg-metal by milling it with Al-chips in a closed reactor. It indeed occurs at RT and gives a pure liquid Hg-metal. That is automatically segregated and collected over the solid Al^{3+} -byproduct of re-oxidized Al-metal formed *in situ*. It does not adhere to the byproduct with its characteristically large angle of contact Θ_c . It is, therefore, easily recovered in a pure metal form with its standard bulk density $\rho = 13.6$ g/cm³. A similar reaction also occurs on milling Al chips in an aqueous Hg^{2+} -solution. We performed a series of batch reactions and successfully recovered a batch of 500 g of pure Hg-metal.

Now, let us comment on the reaction of a thin amalgam film of Al-metal surface. The amalgam inherently adheres to the nascent Al-surface and induces (i) the initial surface oxide, if any, over there and (ii) the $\text{Al} \rightarrow \text{Al}^{3+}$ -cations formed in the amalgamation process as per reaction (2), to segregate and precipitate over the final surface. The co-reduction reaction and subsequent segregation of Al^{3+} -cations occur *in situ* in opposite directions perpendicular to that of the initial Al-metal surface. It results in a directional (along the z axis in Figure 1) intergrowth of the Al-Hg amalgam interface in the Al-surface with a columnar structure of it. The Al^{3+} -impurities and excess amalgam, if any, are washed away, as mentioned earlier in the experimental section. The obtained specimen, therefore, has an extended nascent-Al-surface protected by an extended Al-Hg amalgam interface. The Al-Hg amalgam columns in these competitive reactions are naturally as thinned as possible at an atomic scale according to the experimental conditions.

As shown in Figure 1 *a*, when put in air at RT, the specimen with an extended Al-surface by amalgamation rapidly decomposes/ionizes the O_2 and/or H_2O (from air) into O^{2-} and OH^- anions. The nascent O^{2-} and OH^- anions react with the nascent Al-metal and yield an oxidized/hydrolysed Al^{3+} -product. Here, the Al-Hg amalgam interface produces an activation barrier E_a between the reaction species (A of Al atoms at the Al-surface and B the O^{2-} or OH^- anions above it). The chemical potential μ_e between the reaction species A and B across the interface drives the reaction in a specific direction (AB) perpendicular to the Al-surface (Figure 1 *b*), in a direction opposite to the passage of the air in the reaction. An uninterrupted migration of Al^{3+} cations (from the Al-surface) along AB through the interface produces an uninterrupted columnar growth (through the Al-Hg amalgam channels) of oxidized/hydrolysed Al-metal product. The products therefore are fibres (Figures 2 and 3). A model picture of a fibre growing in *z* direction driven by μ_e is shown in Figure 1 *b*. The length of the uninterrupted reaction defines the length of the fibres in an uninterrupted migration of the reaction species through the interface.

Figure 2 shows the growth of fibres of Al^{3+} -product over an Al-metal surface (catalysed by Hg^{2+} -cations) in air at 305 K (humidity 50%). Figure 2 *a* shows the Al-metal surface just after the reaction started, and demonstrates the discrete nucleation centres of growth of fibres over it. The fibres are 4 to 8 mm long within 180 s of reaction in air (Figure 2 *b*). Fibres of length $L_c = 30$ mm are got in 20 min of the reaction (Figure 2 *c*). As determined from the SEM micrographs, these fibres are very thin with an average diameter $D = 25$ to $60 \mu m$. The D and L_c values of the fibres vary with the experimental conditions of

temperature and humidity of the atmosphere. As shown in Figure 3, fibres of length 15, 30 and 45 mm and diameter 25, 40, and $60 \mu m$ thus have grown at humidity 40%, 60% and 70%, respectively at 305 K. Fibres with large diameters are grown at a high humidity ($\phi = 70\%$) and do not maintain their distinct structures (Figure 3 *c*).

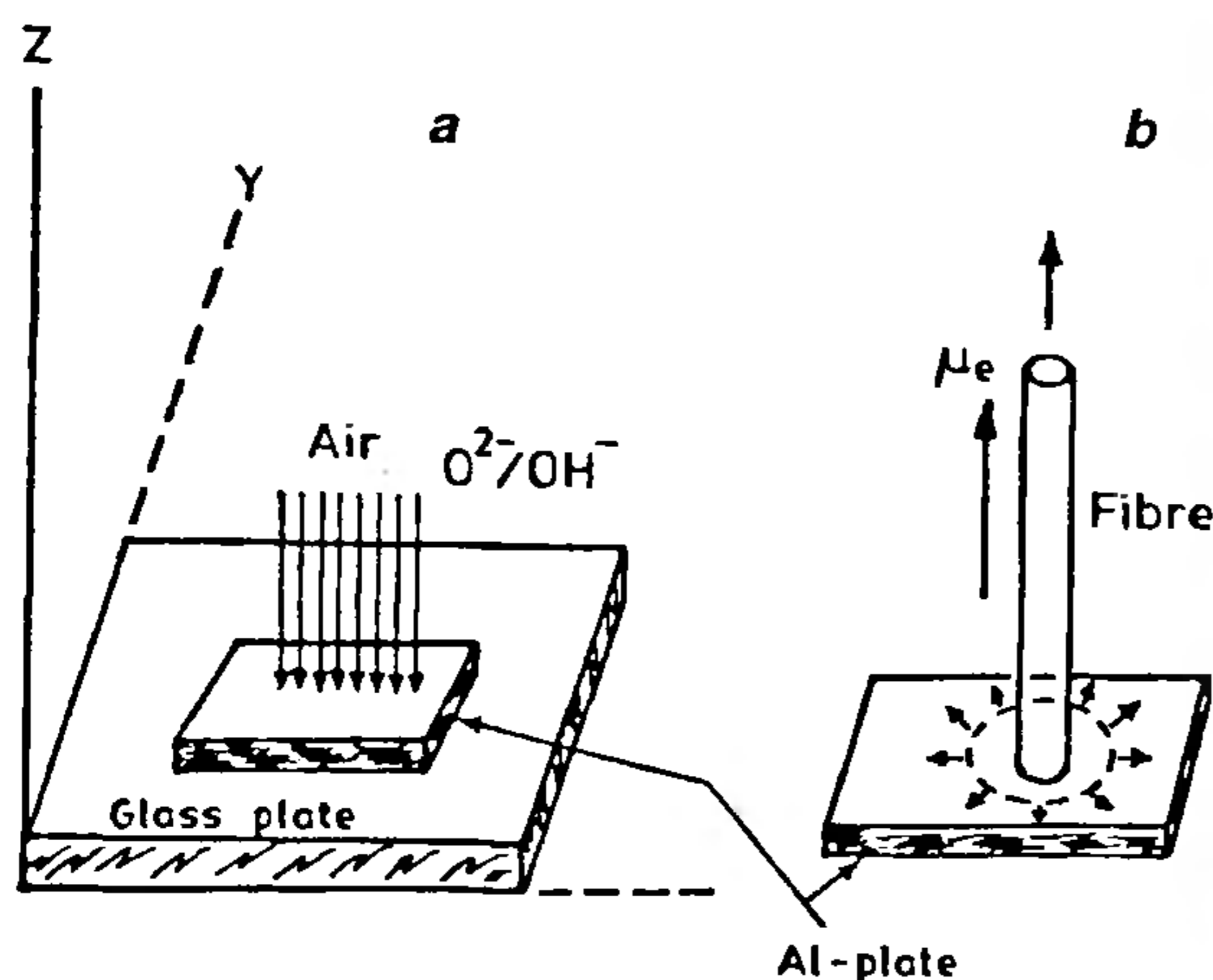


Figure 1. Schematic diagram of surface oxidation of Al-metal catalysed with Hg^{2+} -cations in air. The arrows in *a*, demonstrate passage of the air to the Al-surface during its oxidation in $AlO(OH) \cdot xH_2O$ molecular fibres. The fibres grow in the opposite direction as shown in *b*. The heat released in the reaction flows mainly along the metal surface as shown by the arrows.

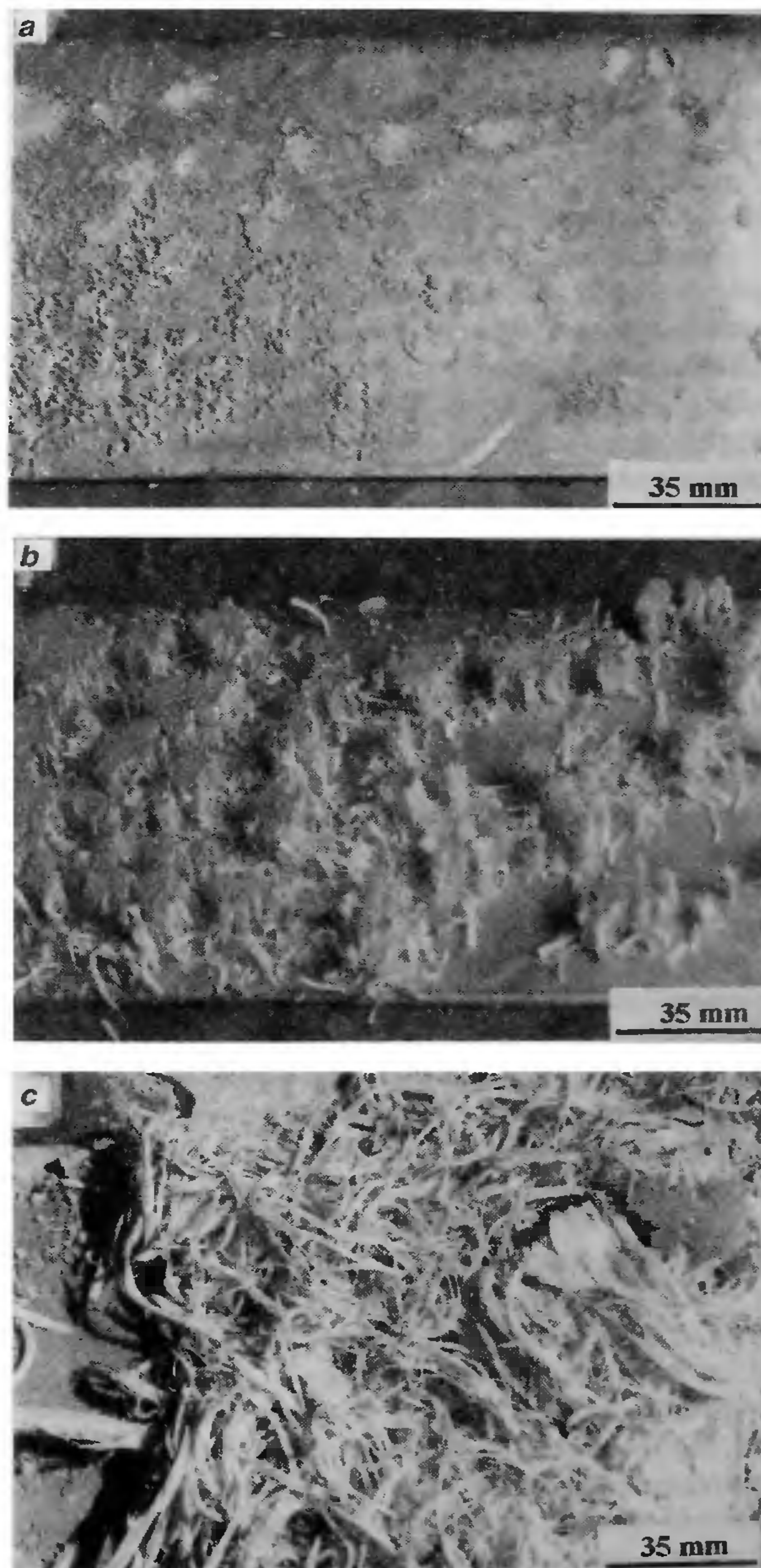


Figure 2. Photographs of $AlO(OH) \cdot xH_2O$ molecular fibres growing at Al-metal surface in air at 305 K at 50% humidity at *a*, 30 s; *b*, 180 s; and *c*, 1800 s of reaction time. Long fibres as 8 mm (*b*) and 30 mm (*c*) are grown with an average diameter of $30 \mu m$.

Model structure of one-dimensional through reaction channels

The reaction and migration of the reaction species occur in divided nucleation centres or micelles. These micelles are caused by the preliminary $\text{Hg}^{2+} \rightarrow \text{Hg}$ co-reduction reaction (2) at the Al-metal surface and amalgamation of the latter with the Hg-metal. In the present example, they control the drift of the reaction species in a specific direction (along the z axis) which is set up perpendicular to the Al-metal surface according to the initial chemical potential in the reaction. The unidirectional migration of the reaction species is indicative of their unidirectional cylindrical model shape of the micelles. These micelles, in fact are cavities or pores caused in the Al-metal surface

due to the loss of Al-metal in the $\text{Hg}^{2+} \rightarrow \text{Hg}$ co-reduction reaction process. The heat released in this highly exothermic reaction, as mentioned earlier, raises the instantaneous temperature T_{ins} at the reaction centre above the average value, T_{av} , of the Al-surface during the reaction. The difference $\Delta T = T_{\text{ins}} - T_{\text{av}}$ leads to a rise in T_{av} to maintain a dynamic equilibrium between the two values. A T_{av} as high as 400 K was recorded without external cooling of the specimen. Thus above a certain critical temperature T_c , the reaction centres become hot spots of the reaction and disrupt it by diminishing (or stopping) the uniaxial drift of the Al^{3+} -cations in it from the Al-metal along the preferred z direction.

In order to confirm the z -directional growth of the nucleation centres, we studied the structure of Al-metal surface before and after an extensive reaction in air. The two structures are compared in Figure 4. The reaction indeed occurs through discrete nucleation centres or reaction channels. They are clearly reflected in discrete fine pores (Figure 4 *a*) of the Al-metal surface taken just after the reaction stated. In this case, the surface oxidation of the sample was suppressed by treating it with an aqueous CrO_3 solution (10^{-4} M) to permit its photograph

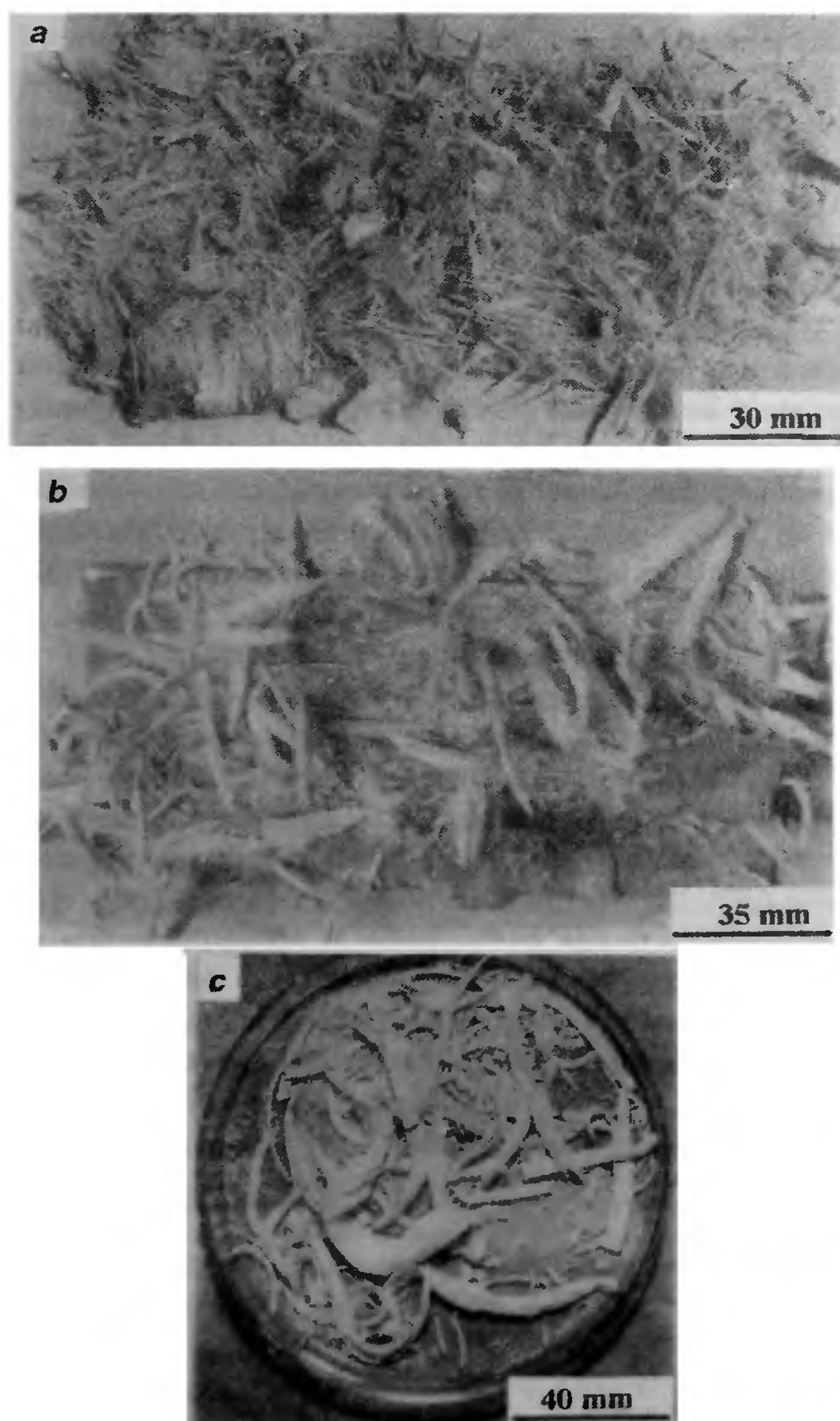


Figure 3. The $\text{AlO(OH).}x\text{H}_2\text{O}$ fibres of lengths 15, 30, and 45 mm and diameters 25, 40, and 60 μm , respectively grown at humidity *a*, 40%, *b*, 60%, and *c*, 70% in air at 305 K.

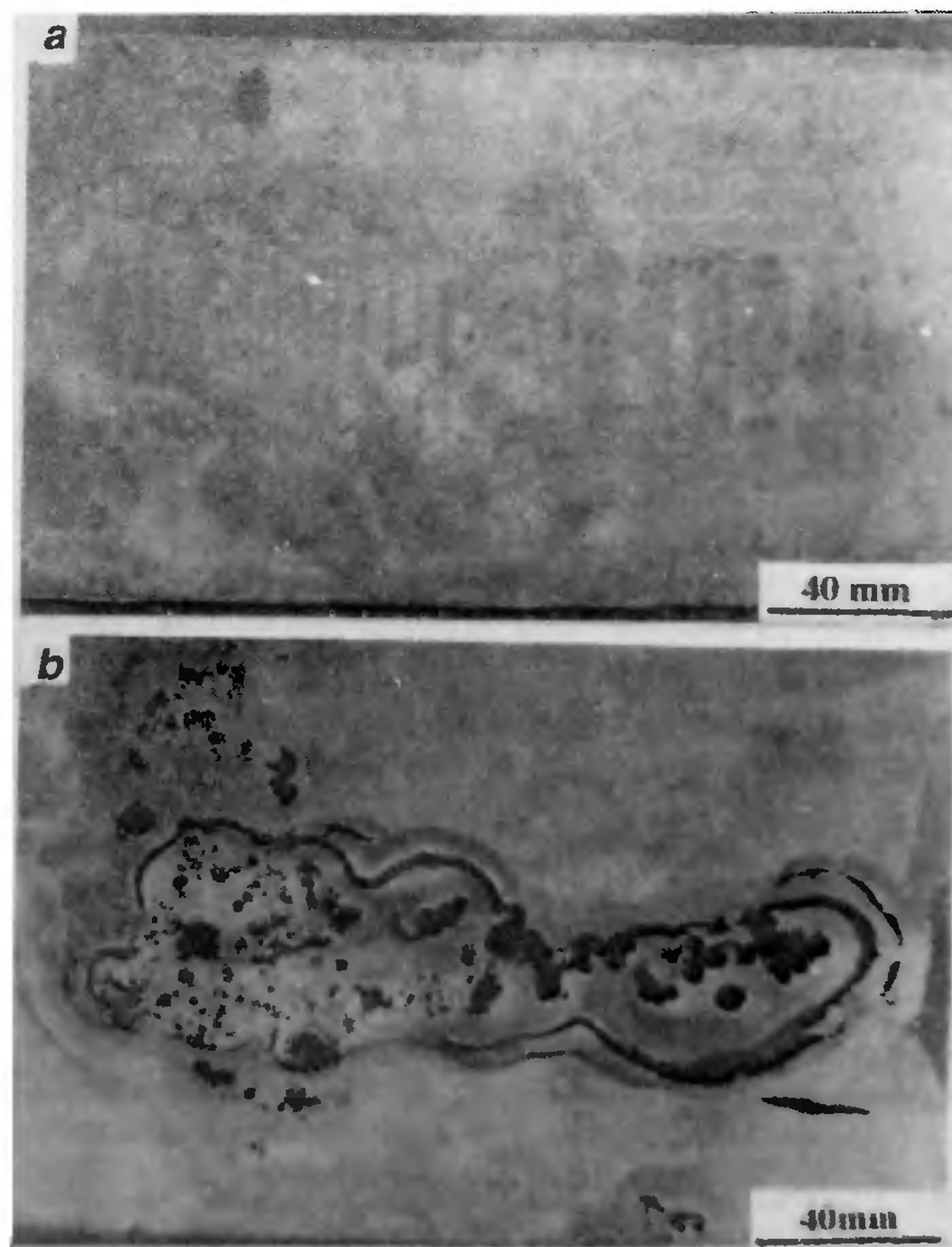


Figure 4. Morphology of *a*, formation of divided oxidation centres at a refreshed Al-metal surface catalysed with Hg^{2+} -cations, and *b*, dissolution of it during its surface oxidation in air.

without much surface oxidation. As the surface oxidation reaction in air proceeds, the pores grow in size perpendicularly downwards in the Al-metal surface and ultimately convert it into elongated pores or through channels with the Al-metal lost in it (reaction). However, in Figure 4, because of an excessive reaction, the presumed original fine pores are recombined in groups in big pores of final diameter as much as 1 mm or even more.

A similar pattern of pores appears in an anodic oxidation of Al-metal surface with one-dimensional channel at a nanometer/micrometer scale¹⁴. The Al-metal membranes obtained with small pores have the potential to act as high performance catalyst, a gas separation membrane and nanocages for constructing novel magnetic and electronic devices^{3,15-18}. The formation of an aligned

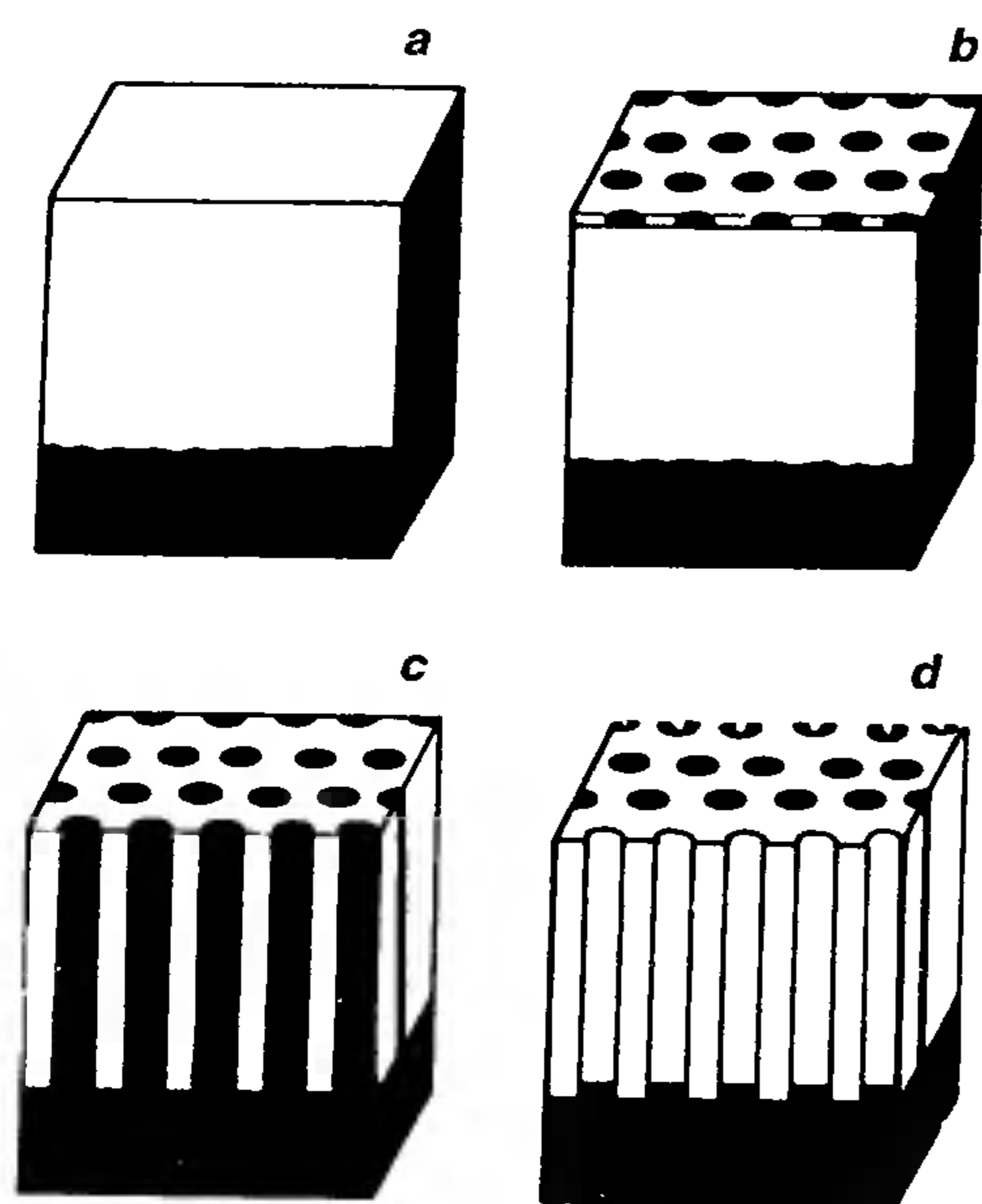


Figure 5. Schematic drawings of the reaction process of Hg^{2+} -cations at Al-metal surface and formation of one-dimensional through channels. *a*, Al-metal surface just after a surface treatment with Hg^{2+} -cations; *b*, nucleation of Hg^{2+} -Al reaction centres at the Al-surface; *c*, growth of one-dimensional through channels of Al-Hg amalgam; and *d*, leaching out of the excess amalgam and oxidized Al-atoms into Al^{3+} -cations in the amalgamation process.

one-dimensional pore along the z axis in this example begins with the $\text{Hg}^{2+} \rightarrow \text{Hg}$ co-reduction reaction at Al-metal surface and amalgamation of it by the Hg-metal in subsequent steps as discussed earlier. This involves a directional $\text{Al} - 3\text{e}^- \rightarrow \text{Al}^{3+}$ co-oxidation reaction of Al-atoms at the Al-metal surface and subsequent precipitation of the Al^{3+} -product through thin Al-Hg amalgam interface along the pores. This is schematically shown in Figure 5. It involves a four-step reaction process of the specimen in air as follows. In the first step a refreshed Al-surface is obtained. This is treated with Hg^{2+} -cations, in the subsequent step and the assumed ion-exchange reaction starts at the surface in discrete centres or micelles shown by the dark circular spots (Figure 5 *b*). The reaction proceeds as a function of time and micelles grow with Al^{3+} intergrowth (Figure 5 *c*) in the surface along the z axis in the next step. As the oxidation of the specimen proceeds by diffusion of Hg^{2+} -cations, the reaction interface moves from the surface perpendicularly downward towards the bottom. As a result, an one-dimensional needle-like regular array of oxidized Al intergrowth in the specimen is formed. In the final step, the needle-like oxidized Al^{3+} -sample is precipitated and leached out (Figure 5 *d*) by washing in a dilute acid and in distilled water.

The specimen obtained with an extended reaction channel is now ready for the scheduled surface oxidation by air in its molecular fibres. The reaction channels (pores) collimate a fast one-dimensional columnar oxidation of the specimen in molecular fibres of the oxidized Al^{3+} -product in air. In this case, the fibre forms an expanded diameter of the pore according to expansion of the specimen from the Al-metal to the final product. Atomic density of Al in the Al-metal is decreased roughly by a factor of $f = 2.5$ on its oxidation in Al_2O_3 and by a factor of $f \sim 5.0$ to that in $\text{AlO}(\text{OH}) \cdot \alpha\text{H}_2\text{O}$. Both involve a large expansion of its volume by an order of magnitude in accordance to their bulk densities ρ . For example, $\rho = 2.70 \text{ g/cm}^3$ in pure Al-metal decreases to $\sim 0.20 \text{ g/cm}^3$ (Table 1) on its oxidation with $\text{AlO}(\text{OH}) \cdot \alpha\text{H}_2\text{O}$. It induces a mechanical stress σ in the specimen during its oxidation as a possible origin of forces between the metal and its oxidized Al^{3+} -product. As the reaction takes place at the pore bottom, the material can only expand in the vertical direction so that

Table 1. Structure parameters of $\text{AlO}(\text{OH}) \cdot \alpha\text{H}_2\text{O}$ molecular fibres grown by surface oxidation of Hg^{2+} -catalysed Al-metal surface in air at 305 K under different experimental conditions of humidity

SI no.	Fibres	Humidity (%)	α value	Structure	Density (g/cm^3) ^a	Length (mm)	Diameter (μm)	Aspect ratio
1	$\text{AlO}(\text{OH}) \cdot \alpha\text{H}_2\text{O}$	40	0.20	Amorphous	0.20	15	25	600
2	$\text{AlO}(\text{OH}) \cdot \alpha\text{H}_2\text{O}$	50	0.25	Amorphous	0.20	30	30	1000
3	$\text{AlO}(\text{OH}) \cdot \alpha\text{H}_2\text{O}$	60	0.30	Amorphous	0.25	30	40	750
4	$\text{AlO}(\text{OH}) \cdot \alpha\text{H}_2\text{O}$	70	0.35	Amorphous	0.30	45	60	750
5	Sample 2 annealed, 2 h at 900 K*	—	—	Crystalline ($\gamma\text{-Al}_2\text{O}_3$)	1.95	2–5	5	400–1000

*The recrystallized fibres on thermal annealing are broken into pieces with reduced diameter by modification in porosity and internal structure.

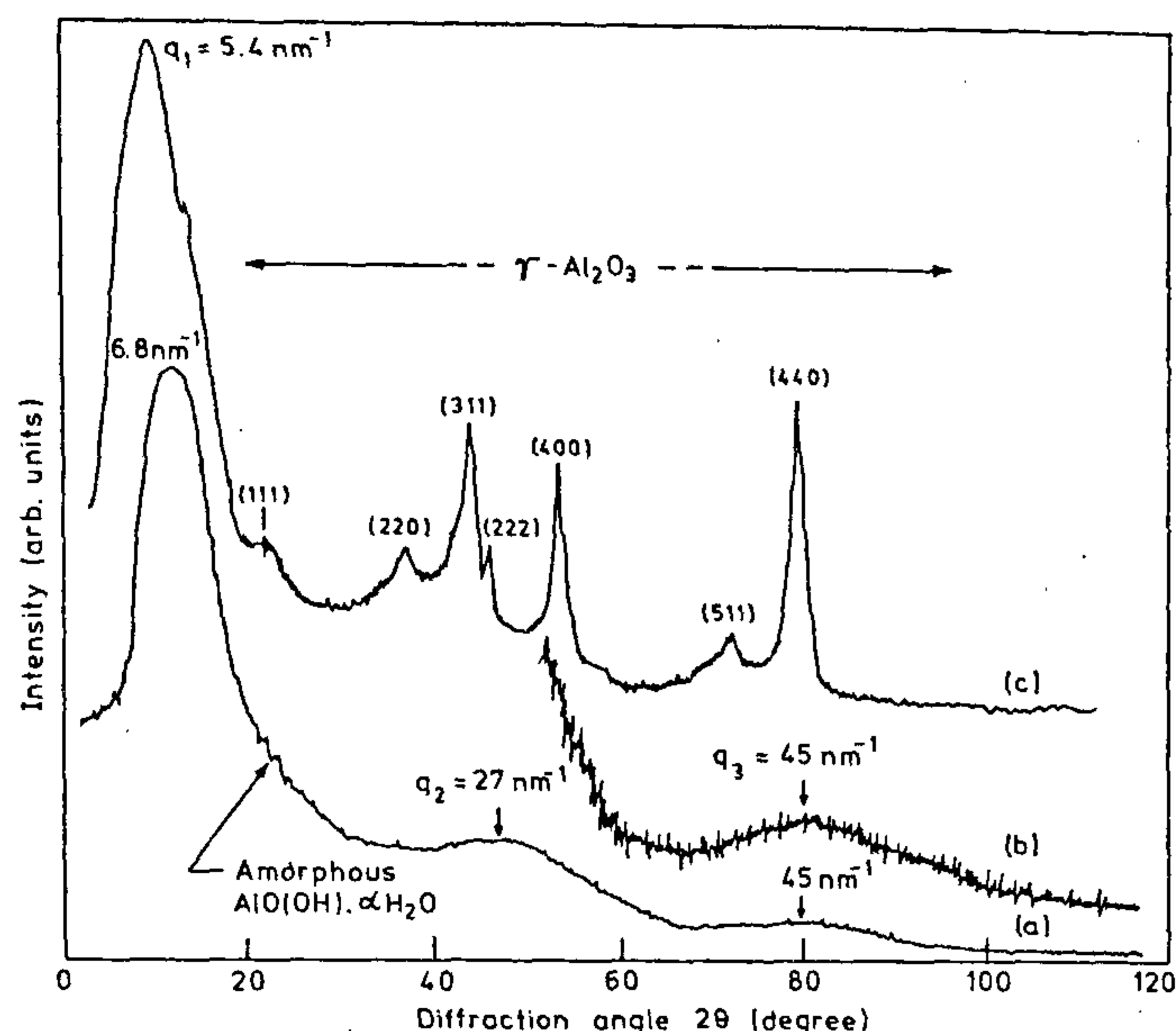


Figure 6. X-ray diffractograms of (a) or, (b) as-received, and (c) recrystallized $\text{AlO(OH)} \cdot \alpha\text{H}_2\text{O}$ fibres in $\gamma\text{-Al}_2\text{O}_3$ at 900 K for 2 h in air. (b) is an expansion of a part of (a) along the y-axis by a factor of ~ 5 . The diffraction peaks in (c) are marked by their (hkl) values.

the existing pore walls are pushed symmetrically upward, leading to the directional growth of the Al^{3+} -product in its molecular fibres. Here, the structure of the pores, therefore, plays a crucial role in driving an ordered growth of fibres through the driving forces of the reaction of (i) the chemical potential μ_e and (ii) the mechanical stress σ , both of which act in the same direction perpendicular to the Al-metal surface.

Composition and amorphous structure of fibres

Figure 6 shows X-ray diffractograms of an as-received Al^{3+} -product of fibres and that is annealed at 900 K for 2 h in air. The received sample which has $\alpha = 0.25$ (Table 1) molecules of H_2O per molecule, exhibits a strong X-ray diffraction halo at wavevector $q_1 = 6.8 \text{ nm}^{-1}$ [where $q_i = (4\pi \sin \theta)/\lambda$] followed by two weak halos at $q_2 = 27 \text{ nm}^{-1}$ and $q_3 = 45 \text{ nm}^{-1}$. The annealed sample is recrystallized in $\gamma\text{-Al}_2\text{O}_3$ with a $\text{O}_4\text{F}_{3\text{DM}}$ cubic crystal structure with lattice parameter $a_0 = 0.79 \text{ nm}$, which is the same as the standard value¹⁹. The diffractogram also has a halo at modified $q_1 = 5.4 \text{ nm}^{-1}$ due to the residual amount of an amorphous Al_2O_3 with a modified structure of a virgin sample as described later.

The half-bandwidth (i.e. the full-width at half peak height) $\Delta 2\theta_{1/2} \sim 10^\circ$, or even larger, in these halos is too large to ascribe them to lattice reflections from small crystallites, $r \geq r^*$, according to the Debye-Scherrer relation²⁰. It predicts a smaller $r \leq 0.8 \text{ nm}$ crystallite size (diameter) than its critical $r^* \geq 2.0 \text{ nm}$ which is defined by $r^* = 4\sigma/\Delta G_v$, with σ the surface-energy and ΔG_v the change in the Gibbs free-energy over its liquid state value^{13,21}. Moreover, according to Bragg's relation,

$2d \sin \theta = \lambda$, the q_1 halo gives $d = \sim 1.0 \text{ nm}$, which is larger than an interatomic distance in this series. These ambiguities are indicative of the fact that the sample is not crystalline. It has an amorphous structure with a small configuration or domains of molecules at a microscopic scale. These microscopic domains behave as strong surface-reflectors to reflect an X-ray beam of λ comparable to their size r from their quantum confined surfaces. The halo observed at $q_1 \approx 6.8 \text{ nm}^{-1}$ is, therefore, the result of this. The microscopic domains have an average $d \sim 1.0 \text{ nm}$ diameter according to the average position of the diffractogram. The other two halos, which are characteristically weaker in intensity, are ascribed to common^{21,22} atomic reflections in an amorphous structure of the sample with two prominent pair distribution functions of atoms.

On heating in a thermal analyser, the sample transforms to Al_2O_3 at 340–600 K with 21% loss in its mass according to its $\text{AlO(OH)} \cdot \alpha\text{H}_2\text{O}$ molecular structure with $\alpha = 0.25$. The result differs from the earlier reports¹⁴ that Al-metal hydrolysis is an electrochemical cell which gives a product of Al_2O_3 directly. As mentioned above, Al_2O_3 deposits a stable layer over the parent Al-metal surface and protects it from its further oxidation. We performed several experiments with Al-metal at temperatures (external) between 275 and 380 K in air and found that the reaction occurs effectively only at low temperatures $T_{av} \leq 320 \text{ K}$. It ceases on raising T_{av} above 320 K. In fact, at $T_{av} > 320 \text{ K}$, the $\text{AlO(OH)} \cdot \alpha\text{H}_2\text{O}$ decomposes into Al_2O_3 and efficiently inhibits further reaction.

Conclusions

A surface passivation free nascent Al-metal surface (catalysed with Hg^{2+} -cations) readily reacts with air and forms $\text{AlO(OH)} \cdot \alpha\text{H}_2\text{O}$ molecular fibres. The fibres are amorphous in nature. It is suggested that the chemical potential μ_e between the reaction species of Al atoms at the Al-metal surface and OH^- ions (deduced by chemical dissociation of H_2O from air at the surface) over it initiates a rapid growth of the product in the form of fibres perpendicular to it. The mechanical stress σ induced in a voluminous expansion of the specimen along μ_e supports their directional growth. It provides a new chemical method for synthesizing a highly pure product of molecular fibres of $\text{AlO(OH)} \cdot \alpha\text{H}_2\text{O}$ or its Al_2O_3 derivatives. In general, the results are useful for understanding and modelling of self-induced surface oxidation of aluminum and similar metals by air or moisture in ambient atmosphere. This knowledge is important for developing an anticorrosion metal surface to inhibit its surface oxidation.

1. Sowman, H. G. and Johnson, D. D., *Ceram. Eng. Sci. Proc.*, 1985, 6, 1221–1230.

2. Ansell, S., Krishnan, S., Weber, J. K. R., Felten, J. J., Nordine, P. C., Beno, M. A., Price, D. I. and Saboungi, M. L., *Phys. Rev. Lett.*, 1997, **78**, 464–466.
3. Mo, S. D. and Ching, W. Y., *Phys. Rev. B*, 1998, **57**, 15219–15228.
4. Suzumura, A. and Xing, Y., *Mater. Trans. JIM*, 1996, **37**, 1109–1115.
5. Loehman, R. E. and Ewsuk, K., *J. Am. Ceram. Soc.*, 1996, **79**, 27–32.
6. Huang, X. and Nicholson, P. S., *J. Am. Ceram. Soc.*, 1993, **76**, 1294–1301.
7. Belmonte, M., Moreno, R., Moya, J. S. and Meranzo, P., *J. Mater. Res.*, 1994, **29**, 179–183.
8. Goodspeed, G. H. and Shmeckpeper, E. R., *J. Compos. Mater.*, 1994, **28**, 1288–1304.
9. Sowman, H. G., *Am. Ceram. Bull.*, 1988, **67**, 1912–1916.
10. Chen, L., Wang, B., Liu, S. and Yan, Y., *J. Am. Ceram. Soc.*, 1996, **79**, 1494–1498.
11. Ram, S., Singh, T. B. and Pathak, L. C., *Phys. Status Solidi A*, 1998, **165**, 151–164.
12. Ram, S., *Appl. Phys. Lett.* (to be published).
13. DeHoff, R. T., *Thermodynamics in Materials Science*, International edition, McGraw-Hill, Singapore, 1993.
14. Jessensky, O., Muller, F. and Gosele, U., *Appl. Phys. Lett.*, 1998, **72**, 1173–1175.
15. Yang, H., Coombs, N., Solokov, I. and Ozin, G. A., *Nature*, 1996, **381**, 589–592.
16. Sun, T. and Ying, J. Y., *Nature*, 1997, **389**, 704–706.
17. Cai, W., Zhang, Y., Jai, J. and Zhang, L., *Appl. Phys. Lett.*, 1998, **73**, 2709–2711.
18. Kon, S., Iwamoto, Y., Kikuta, K. and Hirano, S., *J. Am. Ceram. Soc.*, 1999, **82**, 209–212.
19. JCPDS (Joint Committee on Powder Diffraction Standards) Powder diffraction file 10.425 (ed. McClume, W. F.), International Centre for Diffraction Data, Swarthmore, PA, 1979.
20. Azaroff, L., *Elements of X-ray-Crystallography*, McGraw-Hill, New York, 1968, p. 557.
21. Ram, S., *Phys. Rev. B*, 1990, **42**, 9582–9586; *ibid*, 1995, **51**, 6280–6286.
22. Ram, S., Singh, T. B. and Srikant, S., *Mater. Trans. JIM*, 1998, **39**, 485–491.

ACKNOWLEDGMENT. The authors thank the Aeronautical Research and Development Board, Government of India, for financial support.

Received 13 July 1999; revised accepted 8 October 1999